Nanoscale Res Lett (2006) 1:68–73
DOI 10.1007/s11671-006-9005-9

NANO EXPRESS

Whispering gallery modes in photoluminescence and Raman spectra of a spherical microcavity with CdTe quantum dots: anti-Stokes emission and interference effects

Nikolai Gaponik · Yury P. Rakovich · Matthias Gerlach · John F. Donegan · Diana Savateeva · Andrey L. Rogach

Published online: 25 July 2006

Abstract We have studied the photoluminescence and Raman spectra of a system consisting of a polystyrene latex microsphere coated by CdTe colloidal quantum dots. The cavity-induced enhancement of the Raman scattering allows the observation of Raman spectra from only a monolayer of CdTe quantum dots. Periodic structure with very narrow peaks in the photoluminescence spectra of a single microsphere was detected both in the Stokes and anti-Stokes spectral regions, arising from the coupling between the emission of quantum dots and spherical cavity modes.

Keywords Microcavity · Nanocrystals · Quantum dots · Raman spectroscopy · Anti-Stokes emission

Introduction

Spherical particles of 2–100 μm in diameter can act as three-dimensional optical resonators providing the feedback required for linear and non-linear optical processes such as enhanced Raman scattering [1]. Polymer latex microspheres containing semiconductor quantum dots (QDs) are promising candidates for the development of advanced Raman sources [2], which can extend the available range of semiconductor microlasers [3]. The combination of the high quality factor (Q) and the small mode volume of dielectric microspheres with the tunable emission properties of QDs has made it possible to observe narrow resonant structure in emission spectra [4, 5], to detect the modification of photoluminescence (PL) decay lifetimes [4, 5], enhanced spontaneous emission and lasing [5, 6]. Nowadays the understanding gained from the organization of microspheres is starting to be used to create new materials such as 3D photonic crystals that can function as optical elements in a number of devices. The properties of photonic band gap materials depend sensitively on the microstructure of the sphere packing and on the possibility to create localized states in the optical spectrum. Thus, there is great incentive to control the optical properties and the quality of such building blocks on the level of a single microsphere.

Experimental method

In this work, we have studied the photoluminescence and Raman spectra of a microcavity-QD system consisting of CdTe colloidal QDs coated onto a polystyrene (PS) microsphere. CdTe QDs capped with thioglycolic acid were synthesized in aqueous media as described elsewhere [7]. A colloidal solution of CdTe QDs with a PL maximum at 620 nm (2.4 nm radius) (Fig. 1) and a PL quantum efficiency of ~25% at room temperature was used for coating PS microspheres with

N. Gaponik
Physical Chemistry/Electrochemistry, TU Dresden, 01062 Dresden, Germany

Y. P. Rakovich (✉) · M. Gerlach · J. F. Donegan
Semiconductor Photonics Group, School of Physics, Trinity College, Dublin 2, Ireland
e-mail: Yury.Rakovich@tcd.ie

D. Savateeva
Brest State Technical University, 224017 Brest, Belarus

A. L. Rogach
Department of Physics and CeNS, University of Munich, 80799 Munich, Germany

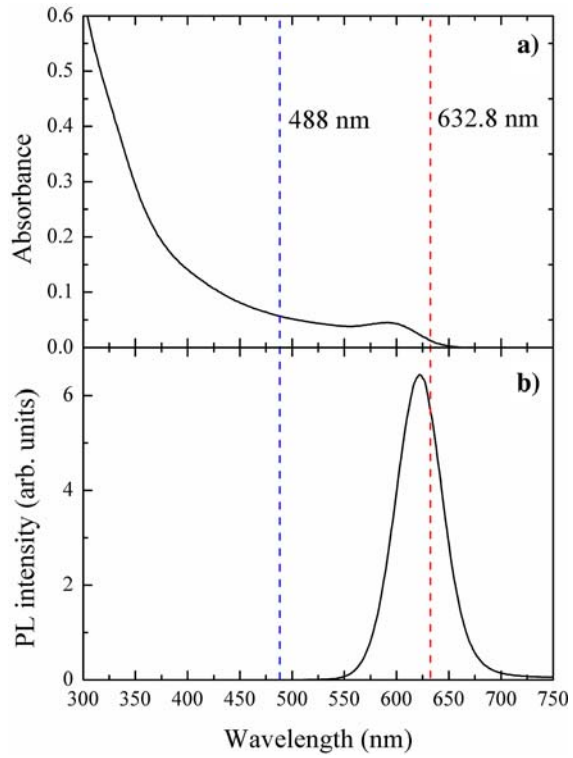

Fig. 1 Room temperature absorption and PL spectra of CdTe NCs in water. Dashed lines indicate the excitation wavelength used in micro-PL and Raman experiments

a monolayer of QDs utilizing the layer-by-layer deposition technique [8]. The diameter of the PS spheres used was 70 microns. Absorption and PL spectra of aqueous solutions of colloidal QDs were measured using Shimadzu-3101 and Spex Fluorolog spectrometers, respectively. The Raman spectra from a single microsphere were recorded in a backscattering geometry using a Renishaw micro-Raman system (~1,800 mm^{-1} grating, 1 cm^{-1} resolution). For all measurements, the microspheres were deposited on a Si wafer, which provides the built-in standard of the Si transverse optical (TO) mode at 520 cm^{-1}. PL and Raman spectra of single microspheres were excited by the 488 nm line of an Ar^+ laser with a power of 2 mW or a He–Ne laser at 632.8 nm with a power up to 3 mW.

Results and discussion

The optical spectra of colloidal CdTe QDs in water are presented in Fig. 1, demonstrating the high optical quality by the pronounced peak in absorption and a single band edge PL band. The blue shift of the QDs absorption band by ~610 meV with respect to bulk CdTe indicates a strong electronic quantum confinement effect.

In contrast to the broad, featureless PL band in the spectra of colloidal QDs (Fig. 1), the emission spectra of a single PS/CdTe microsphere exhibit a tiny ripple structure (Fig. 2, curve 1), which is superimposed on a broad background signal. The spectrum also shows a number of sharp peaks, which are intrinsic to the Raman signal from the PS [9].

Figure 3a shows an enlargement of the measured PL spectrum where the periodic structure of WGM peaks can be seen in more detail, demonstrating that the modes in the PL spectrum are arranged in pairs of two pronounced peaks one of higher intensity and a second smaller peak. Moreover, a few extra tiny peaks can be distinguished in the spectral region between them. To gain more insight into the WGM structure in the microcavity we carried out a fast Fourier analysis, which makes it possible to investigate the periodicity more thoroughly. In the spectral frequency interval 0–3.5 nm^{-1}, we observed strong peaks corresponding to a periodicity of 1.31, 0.65, 0.44 and 0.33 nm (see bars in Fig. 3b). The highest periodicity value could be assigned to the free spectral range (FSR) between modes of the same polarization with radial order numbers $n = 1$. Because transverse electric modes (TE) have normally a higher quality factor than transverse magnetic (TM) modes, we can attribute the stronger peaks in Fig. 3a to the TE modes of the WGM. The good agreement between the measured FSR of 1.32 nm between the TE modes supports this hypothesis. In turn, the periodicity of 0.65 nm is attributed to the FSR between modes of different polarizations (i.e. between

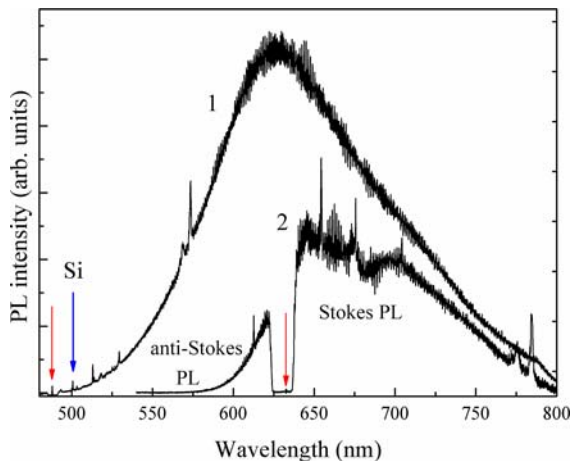

Fig. 2 Room temperature PL spectra from a single PS microsphere coated by one monolayer of CdTe QDs excited by an Ar^+ laser (above band-gap excitation, $\lambda = 488$ nm, curve 1) and a He–Ne laser (below band-gap excitation, $\lambda = 632.8$ nm, lower curve 2). The anomalous decrease of the PL intensity in the wavelength region from 626 to 640 nm is due to the notch filter used. Excitation wavelengths are indicated by red arrows

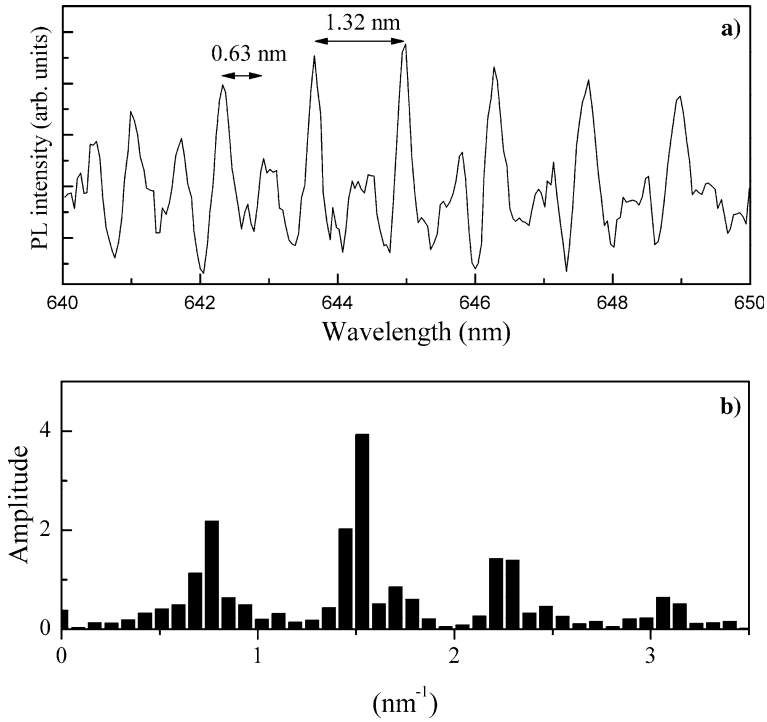

Fig. 3 (**a**) Expansion of the measured fluorescence spectrum. Arrows indicate the free spectral range (FSR) and TE/TM mode splitting. (**b**) Result of fast Fourier analysis

adjacent TE and TM modes) again in agreement with measured modes separation (Fig. 3a). Periodicities of 0.44 and 0.33 nm, obtained from the Fourier analysis, are indicative of the TE and TM modes with radial order numbers which are greater than 1.

We also studied the optical behavior of the microcavity-quantum dot system with excitation below the band gap of the CdTe QDs in the region of low absorption. In addition to the normal Stokes-shifted luminescence, we make the observation of anti-Stokes emission. The tail of the anti-Stokes PL (ASPL) can be seen ranging up to (~200 meV) above the excitation energy (Fig. 2, curve 2). The ASPL process is certainly highly efficient having an intensity comparable to the Stokes PL as seen from Fig. 2. We found that the integrated intensity of ASPL has an almost linear dependence on the excitation intensity under weak or moderate excitation (<200 W/cm^2). This dependence is very similar to the behavior of ASPL in colloidal CdTe QDs where the progressive transition from Stokes PL into ASPL can be observed when changing the excitation wavelength to below the band-gap region [10]. A similar effect was recently reported in small (2 μm) microspheres with a thin shell of semiconductor nanocrystals, and explained by multiphonon-assisted excitation of an electron from the ground state to the excited state through the mediation of the shallow trap levels [2]. In the case of colloidal QDs such a low cross-section mechanism, like anti-Stokes excitation can be only efficient in samples with high enough quantum yields [11, 12]. The observation of ASPL from a PS microsphere with a *single layer* of CdTe QDs which have an order of magnitude lower quantum efficiency than the colloidal dots can be attributed to the optical feedback via the microcavity with a WGM structure which leads to an increased probability of energy transfer to the emitting species. As a result, strong coupling between photonic states of the spherical microcavity and electronic states of CdTe QDs can be achieved simultaneously in both Stokes and anti-Stokes spectral regions (Fig. 2, curve 2). Although anti-Stokes PL was reported for colloidal solutions of highly-luminescent CdTe and CdSe QDs [10, 12, 13] the observation of up-converted PL for a *single* monolayer of close-packed QDs is scarce [2].

As discussed above, Raman scattering from the PS gives a significant contribution to the PL spectra shown in Fig. 2. In order to investigate the microcavity effect on phonon spectra we have studied the Raman scattering from a *single* CdTe layer on a PS microsphere at different excitation conditions.

The measured Raman spectra at resonance excitation by an Ar^+-laser (488 nm) shows a number of peaks which are intrinsic to the PS (220, 620, 759, 793, 1,001 and 1,031 cm^{-1}) (Fig. 4a, b). In addition to these lines, the cavity-induced enhancement of the Raman scattering allows for the observation of the LO phonon mode from only a monolayer of CdTe QDs (166.0 cm^{-1}) (Fig. 4a, b), the mode is redshifted due to confinement of optical phonons [14]. It is noteworthy that we were

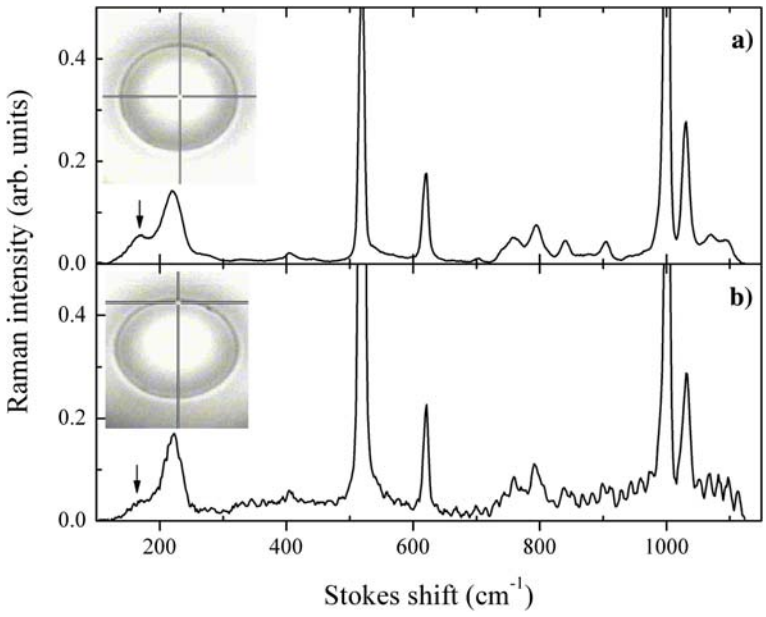

Fig. 4 The Raman spectra of a single CdTe/PS microsphere on a Si substrate (excitation at the center (**a**) and at the rim of a spherical particle (**b**)). Excitation by Ar^+ laser $\lambda = 488$ nm. The insets show microscope images of the CdTe/PS microsphere. The dark cross indicates the excitation position. Arrows indicate the LO phonon mode from a monolayer of CdTe QDs

not able to observe any Raman signal arising from a monolayer of CdTe QDs directly deposited on top of the Si wafer. However, the most remarkable experimental observation is a periodic (ripple) structure with very narrow regular peaks in the spectra of the PS/NCs microsphere, which can be clearly seen in Fig. 4b. This structure corresponds to the WGM modes of the spherical microcavity and can best be detected by providing excitation at the rim of the microsphere.

The observed difference in the efficiency of the WGM peaks at excitation in the center and at the rim of the microsphere can be explained by the spatial distribution of the electro-magnetic field inside the microsphere. The resonant internal field of a spherical cavity corresponding to high-Q modes is mostly confined to the near-surface interior of the microsphere [15]. Therefore, a uniform intensity distribution within the rim of the microsphere in the volume determined by the WGM can be expected if the incident wave is resonant with a WGM. In such a situation edge illumination with a focused beam excites the WGM of a microsphere more uniformly and more efficiently than at central excitation [15] which is in good agreement with our experimental results.

As indicated above, for all measurements the microspheres were deposited on a Si wafer, which can function also as a mirror reflecting the excitation beam. On the other hand, the observation of WGM in spectra of single microcavity testify to the high optical quality of the microsphere surface. Combination of these two modalities can be used to produce an interference patterns with shape and fringe spacing depending on the excitation geometry. Figure 5 shows the interference patterns recorded when excitation light was focused on the top of a spherical microcavity and just outside the rim of the microsphere. The resultant interference light is generated by multiple reflections between the microsphere surface and the Si wafer surface. As the excitation spot shifts well off the microsphere rim, the number of interference fringes increases. We believe that the observed phenomenon can be used for the development of optical encoders that can determine the precise position of a microparticles above a reflecting interface.

Another feature, which can be clearly seen in Fig. 4b is that the intensity of WGM peaks decreases as they approach the excitation wavelength. We suggest that the observed reduction of the peaks intensity in the spectra of a CdTe/PS microsphere is due to absorption by QDs that are coupled to the relevant WGM. It is well- known that absorption or gain or refractive index variation alter the Q value of the spherical microcavity [16]. Because of the Stokes shift (30 nm) between the intrinsic PL peak and the absorption peak of the CdTe QDs, the absorption coefficient is reduced on the long-wavelength part of the PL band (Fig. 1), allowing a higher Q factor to be achieved in this spectral region.

Gaining a better insight into these experimental findings, we have studied spectra of CdTe/PS microspheres using low intensity non-resonance excitation by a He–Ne laser. In that case, strong coupling between the WGM of the spherical microcavity and the electronic states of the CdTe QDs was achieved resulting in an *enhanced luminescence contribution* to the signal simultaneously in both the Stokes and

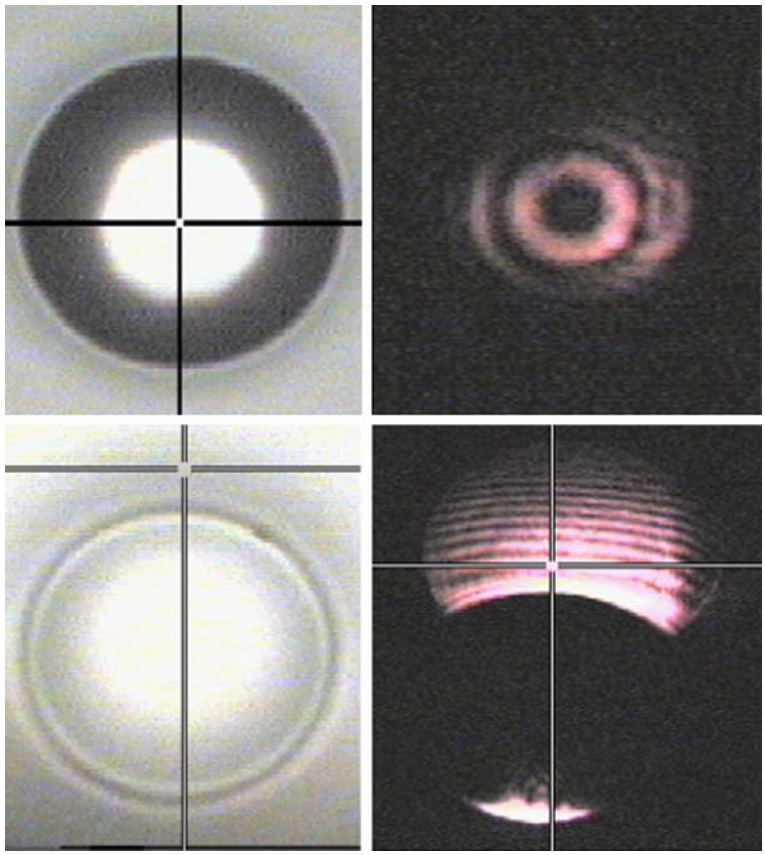

Fig. 5 Microscope images of the CdTe/PS microsphere on a Si substrate and the corresponding interference images. The dark cross indicates the excitation position

anti-Stokes spectral regions (Fig. 6). Both down and up-converted PL emissions from QDs and WGM are dominant in the spectra, while the Stokes and anti-Stokes Raman signals from the Si TO modes arising from substrate have a relatively small contribution.

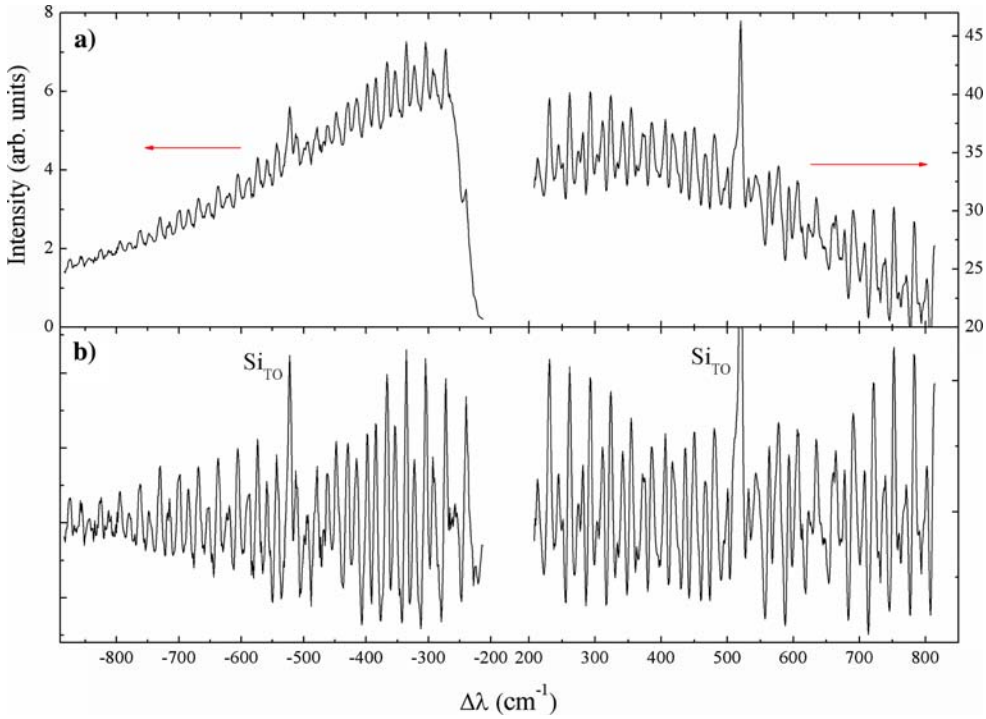

Fig. 6 Room temperature spectrum of a single PS/CdTe microsphere on a Si substrate. Excitation by HeNe laser $\lambda = 632.8$ nm before (**a**) and after (**b**) PL background subtraction

The anti-Stokes process is certainly highly efficient having an intensity about 5% of the Stokes signal as shown in Fig. 6. The observation of an anti-Stokes enhanced signal from a CdTe/PS microsphere once again can be attributed to the optical feedback via the microcavity with a WGM structure. The observed spectra show a sequence of sharp peaks, which only occur at discrete frequencies depending on the refractive index n_s and the radius R of the microsphere. The modes in the spectrum in Fig. 6 are arranged in pairs of two pronounced peaks where the TE mode corresponds to the peak with higher intensity and the TM mode to the smaller peak, which follows from polarization experiments. Calculations based on Mie theory allow a comparison with the experimental data. The spacing is measured between the first and the second peak, respectively, of two adjacent pairs. The analytical equation using expansions of the Bessel functions is valid for large spheres with the radius $R \gg \lambda$ [17]. The FSR v_f is given by

$$v_f = \frac{c}{2\pi n_s R}, \tag{1}$$

where c is the speed of light. The wavelength dependence of the refractive index for a PS microspheres is given by the dispersion relation

$$n_s = A + \frac{B}{\lambda^2} + \frac{C}{\lambda^4} \tag{2}$$

with $A = 1.5656$, $B = 0.00785$ and $C = 0.000334$. With these two equations, the expected wavelength-dependent spacing of the WGMs was calculated. The calculations show a good agreement with the experimental data. Within the region of the measured spectrum, the spacing ranges from 1.11 nm for the WGMs at around 602 nm corresponding to a Stokes shift of 802 cm^{-1} up to 1.37 nm at 667 nm or 812 cm^{-1}. Within the spectral range of 65 nm the spacing increases about 0.25 nm due to the dispersion of the PS refractive index. Accordingly, Eqs. (1) and (2) allow us to choose the desired mode spacing by calculating the appropriate size of the microsphere.

Because of the very high PL quantum efficiency of QD's, the WGM peaks in the spectra (Fig. 6a) are superimposed on a broad background PL signal. In order to show more clearly the WGM structure itself, this background has been subtracted using a multi-Gaussian function (Fig. 6b). This procedure revealed one more feature which is typical for spherical microcavities, a slowly oscillating structure caused by interference between light diffracted and transmitted at the poles of the microsphere [18]. As can be seen in Fig. 6b, the WGM peaks are in fact grouped together and a periodic interference structure can be clearly seen both in Stokes and anti-Stokes spectral regions with a period of ~340 and ~230 cm^{-1}, respectively. Although theoretically predicted for an elastic scattering experimental geometry, this phenomenon has not been reported for PL experiments so far.

In conclusion, PL and Raman spectra from a monolayer of CdTe quantum dots were observed due to strong coupling with the spherical microcavity. Simultaneous Stokes and anti-Stokes emission were realized by low intensity excitation below the band gap. Recently, a microcavity-based Raman laser with an ultrahigh-Q silica microsphere was demonstrated based on WGM Raman Stokes scattering [4]. In this paper we show that using colloidal QDs it is possible to provide multiplexing of the optical signal both in the Stokes and anti-Stokes spectral regions, with controllable peak spacing.

Acknowledgments This work was supported by Science Foundation Ireland (SFI) under grant number 02/IN.1/I47. ALR acknowledges the Walton Award from the SFI.

References

1. K.J. Vahala, Nature **424**, 839 (2003)
2. Y.P. Rakovich, J.F. Donegan, N. Gaponik, A.L. Rogach, Appl. Phys. Lett. **83**, 2539 (2003)
3. S.M. Spillane, T.J. Kippenberg, K.J. Vahala, Nature **415**, 621 (2002)
4. X.D. Fan, M.C. Lonergan, Y.Z. Zhang, H.L. Wang, Phys. Rev. B **64**, 115310 (2001)
5. M.V. Artemyev, U. Woggon, R. Wannemacher, H. Jaschinski, W. Langbein, Nano Lett. **1**, 309 (2001)
6. V.I. Klimov, M.G. Bawendi, MRS Bull. **26**, 998 (2001)
7. N. Gaponik, D.V. Talapin, A.L. Rogach, K. Hoppe, E.V. Shevchenko, A. Kornowski, A. Eychmuller, H. Weller, J. Phys. Chem. B **106**, 7177 (2002)
8. A.S. Susha, F. Caruso, A.L. Rogach, G.B. Sukhorukov, A. Kornowski, H. Möhwald, M. Giersig, A. Eychmüller, H. Weller, Coll. Surf. A **163**, 39 (2000)
9. M. van den Brink, M. Pepers, A.M. van Herk, J. Raman Spectrosc. **33**, 264 (2002)
10. Y.P. Rakovich, S.A. Filonovich, M.J.M. Gomes, J.F. Donegan, D.V. Talapin, A.L. Rogach, A.Eychmüller, Phys. Stat. Sol. (b) **229**, 449 (2002)
11. K.I. Rusakov, A.A. Gladyshchuk, Y.P. Rakovich, J.F. Donegan, S.A. Filonovich, M.J.M. Gomes, D.V. Talapin, A.L. Rogach, A. Eychmüller, Opt. Spectr. **94**, 921 (2003)
12. X. Wang, W.W. Yu, J. Zhang, J. Aldana, X. Peng, M. Xiao, Phys. Rev. B **68**, 125318 (2003)
13. W. Chen, Chem. Phys. **122**, 224708 (2005)
14. M. Gorska, W. Nazarewicz, Phys. Stat. Sol. (b) **65**, 193 (1974)
15. A. Serpenguzel, S. Arnold, G. Griffel, J.A. Lock, J. Opt. Soc. Am. B **14**, 790 (1997)
16. Y.P. Rakovich, L. Yang, E.M. McCabe, J.F. Donegan, T. Perova, A. Moore, N. Gaponik, A. Rogach, Sem. Sci. Techn. **18**, 914 (2003)
17. S. Schiller, R.L. Byer, Opt. Lett. **16**, 1138 (1991)
18. P. Chylek, J. Zhan, J. Opt. Soc. Am. A **6**, 1846 (1989)